scientific reports

Check for updates

OPEN

Different concentrations of 2-Undecanone triggers repellent and nematicidal responses in *Caenorhabditis elegans*

Wei Dai[1], Yile Zhai[2], Fan Yang[1], Wen Chen[1], Chen Liu[1], Yaru Tian[1], Feng Huang[1], Minmin Cai[1], Longyu Zheng[1], Wanli Cheng[3], Weidong Chen[4] & Jibin Zhang[1]✉

The compound 2-undecanone is widely distributed in the natural environment and exhibits a dual-action mechanism against nematodes. It demonstrates repellency and contact toxicity against both *Caenorhabditis elegans* and *Meloidogyne incognita*. However, research on the dual-function mechanism of 2-undecanone remains relatively limited. In this study, using chemotaxis experiments, we found that 2-undecanone (at concentrations of 1–5 mg/mL) signal is detected through AWB olfactory sensory neurons in nematode, and then transduced through the cGMP pathway to induce repellent behavior. Moreover, we observed that 2-undecanone (at concentrations of 0.06–0.08 mg/mL) induces intracellular calcium accumulation and causes lysosomal membrane rupture. We further identified Hsp70 A and V-ATPase A as the targets of 2-undecanone responsible for its contact killing effect. Furthermore, 2-undecanone was found to alter sphingomyelin metabolism in both wild-type *C. elegans* and *hsp-1* mutants. This alteration led to decreased acid sphingomyelinase activity, reduced ceramide levels, and increased sphingomyelin levels. These results indicated that 2-undecanone has dual functions and two target receptors Hsp70 A and V-ATPase A against nematodes, and one AWB olfactory neuron repelled nematodes. The dual-action mode of 2-undecanone can decrease the nematodes' tolerance to the compound appropriately, extending its efficacy duration. Understanding the dual function mechanism of action of 2-undecanone will aid in devising innovative approaches for managing nematode control.

Keywords 2-Undecanone, *C. elegans*, Repellent olfaction, Lysosome integrity, Hsp70 A, V-ATPase A.

Root-knot nematodes (RKNs) pose a severe threat to over 5500 plants worldwide, including field and horticultural crops and vegetables, causing significant economic losses annually[1]. *Meloidogyne incognita* is among the most damaging nematodes[2]. For a long time, RKNs controlling has relied on chemical nematicides. The emergence of bio-formulations has led to development of greener and environment friendly nematicides[3–5]. Due to their advantages, biological methods for controlling RKNs have been the focus of increasing research. Many microorganisms and their metabolic products have been reported to have good nematode control activity[6,7]. However, the mechanism by which microbial metabolites prevent nematodes is not yet clearly understood.

Caenorhabditis elegans is a model worm to evaluate volatiles as molecular pattern to regulate host response. The detection of volatile organic compounds (VOCs) relies on chemosensory neurons, which then trigger responses of attraction or repulsion. Attractive VOCs are recognized by AWA or AWC neurons, while repulsive VOCs are identified by AWB neurons[8]. The majority of odorant receptors typically belong to the family of G protein-coupled receptors (GPCRs) in *C. elegans*[9]. The volatile organic compound 1-undecanone, produced by *Pseudomonas aeruginosa* PA 14, is detected by AWB neurons, leading to aversive behavior and eliciting an immune response[10]. The volatile metabolite Furfural acetone from *Paenibacillus polymyxa* KM2501-1 attracts

[1]National Key Laboratory of Agricultural Microbiology, College of Life Science and Technology, National Engineering Research Center of Microbial Pesticides, Huazhong Agricultural University, Wuhan 430070, China. [2]The Second Hospital, Cheeloo College of Medicine, Shandong University, Jinan 250033, Shandong, China. [3]State Key Laboratory of Biocatalysis and Enzyme Engineering, School of Life Science, Hubei University, Wuhan 430062, Hubei, China. [4]Department of Plant Pathology, Washington State University, 99164-6430 Pullman, USA. ✉email: zhangjb@mail.hzau.edu.cn

nematodes, which is sensed depending on the multiple receptors such as GPCRs SRA-13 of AWA neurons and STR-2 of AWC neurons in *C. elegans*[11].

Lysosome-related research has revealed the crucial roles that lysosomes play in cellular stress responses and the regulation of lifespan[12]. Lysosomes are cytoplasmic single-membrane organelles containing over 60 hydrolytic enzymes, which degrade materials introduced through endocytosis, phagocytosis and autophagy. Many of these enzymes are activated by the acidic pH of the lumen, which is generated and maintained by lysosomal V-ATPase[13,14]. The rupture of lysosomal membrane results in the release of the contents into the cytoplasm[15]. In the cytoplasm, the role of cathepsins in the execution of cell death is unknown. Although lysosomal cell death (LCD) can occur independently of caspases, cytoplasmic cathepsins can cleave the pro-apoptotic protein Bid. This action promotes the mitochondrial translocation of pro-apoptotic proteins Bax and Bak, leading to mitochondrial membrane permeabilization and ultimately inducing caspase-dependent apoptosis[16].

While the integrity of the lysosomal membrane is crucial to cell viability[17], the mechanism by which it is maintained in *C. elegans* is not fully understood. In mammalian cells, Hsp70 stabilizes lysosomes by tightly and selectively binding to bis(monoacylglycero)phosphate (BMP), which in turn promotes the binding and activity of acid sphingomyelinase (ASM) in acidic environments[18]. Calpain activation, with a concomitant decrease in the lysosomal membrane localization of Hsp70.1 and BMP levels, can diminish Hsp70.1-BMP binding, resulting in decreased ASM activity and lysosomal rupture and leakage of cathepsin B into the cytosol. These results suggest that at least in some systems, regulation of ASM activation by Hsp70.1-BMP affects lysosomal stability and cell survival or death[18]. SCAV-3, the homologue of human LIMP-2 in *C. elegans*, has been identified as a pivotal regulator of lysosomal characteristics[19]. However, it remains unknown whether Hsp70 plays a role in maintaining lysosomal membrane integrity of *C. elegans*.

In a previous study we identified 2-undecanone, a volatile organic compound from the fermentation broth of *Paenibacillus polymyxa* KM2501-1[6], as being strongly nematocidal and repellent to *Meloidogyne incognita*, but the underlying mechanisms of these dual functions are unclear. 2-Undecanone is a medium-chain methyl ketone consisting of 11 carbon atoms, and can be produced by a variety of plants, animals and microorganisms[20]. Thus, we used *C. elegans* as a model to explore its mechanism of action in terms of both repellency and nematicide effect in this study.

Results

2-Undecanone is sensed by AWB odor sensory neurons of *C. elegans*

2-Undecanone has been found to have excellent antagonistic activity against *Meloidogyne incognita*, including contact killing and repellency[6]. To investigate the mechanism of its action, we used the free-living model organism *Caenorhabditis elegans* for conducting experiments (Fig. 1A). An experiment device (Fig. 1B) was made to test the behavior of nematodes to 2-undecanone. Worms preferred to avoid 2-undecanone and crawl to the opposite side, with chemotaxis index of -0.11 and − 0.21 at concentrations of 1 mg/mL and 5 mg/mL, respectively, compared to chemotaxis index of 0.02 of the control group (0 mg/mL of 2-undecanone) (Fig. 1C). The results indicated that 2-undecanone has the potential to repel nematodes to achieve the purpose of nematode prevention in agricultural fields.

To check whether olfaction in worms is necessary for sensing 2-undecanone, we tested the chemotaxis response of various *C. elegans* mutants to the 2-undecanone at the optimal concentration of 5 mg/mL (Fig. 1D). The mutants in *lim-4 (ky403)*, which are deficient in functional AWB neurons[21], showed no response to 2-undecanone. *odr-7 (ky4)* worms lacking functional AWA neurons[22,23] showed a normal aversion response to 2-undecanone with a chemotaxis index of -0.12. These results indicated that sensing of 2-undecanone is dependent on functional AWB neurons.

Stimulation in AWB neurons can activate signaling cascades[24,25]. The downstream signaling pathways of most olfactory neurons are cGMP-mediated, including the AWB neurons[10 22]. We tested mutants in *tax-2 (p671) /tax-4 (e2861)*, *odr-1(n1936)* and *daf-11 (m47)*, which belong to the cGMP signaling pathway and the CNG channel, for their effects on chemotaxis to 2-undecanone. The results indicated that repellency responses of mutant nematodes in genes *tax-2 (p671)*, *tax-4 (e2861)*, *odr-1(n1936)* and *daf-11 (m47)* to 2-undecanone were all significantly weaker compared with WT nematodes. These showed that the cGMP pathways are essential for signal transduction process in nematode detecting 2-undecanone.

2-Undecanone caused lysosomal rupture in *C. elegans*

We also found that 2-undecanone is highly nematicidal at concentrations of 60 and 80 μg/mL against the *C. elegans* (Fig. 2A). To explore the molecular mechanism of this nematicidal activity, we investigated whether 2-undecanone causes necrosis in *C. elegans*. Because necrosis is characterized by the rupture of lysosomes[26], we first used the specific marker Lyso-Tracker to regulate lysosomal integrity in vitro. Treatment with 2-undecanone showed a burst of red fluorescence (Fig. 2B), as well as in heat shock treatment, consistent with lysosomal rupture. Next, we examined lysosomal integrity in vivo with strain pwIs50, a transgenic strain of *C. elegans* expressing the specific marker LMP-1::GFP. Treatment with 2-undecanone or heat shock resulted in diffusion of GFP-labeled lysosomal debris throughout the cell cytosol (Fig. 2C), providing additional evidence of lysosomal rupture. Furthermore, given that elevated intracellular calcium levels can trigger the activation of cathepsin within the lysosome, ultimately leading to cell necrosis, we utilized the calcium indicator Fluo-4 AM in vitro to evaluate changes in calcium concentration after exposure to 2-undecanone or heat shock. Both treatments resulted in increased fluorescence of calcium (Fig. 2D). Additionally, calcium uptake was also detected in vivo via fluorescence–resonance energy transfer (FRET) in the transgenic strain rnyEx109, which expresses the calcium indicator d3cpv. Compared with the FRET ratio of untreated controls, the ratio with 2-undecanone treatment was significantly higher (Fig. 2E), indicating an increased calcium concentration. Together, in vitro and in vivo assays indicated that 2-undecanone caused an increase in cytoplasmic calcium leading to necrosis in

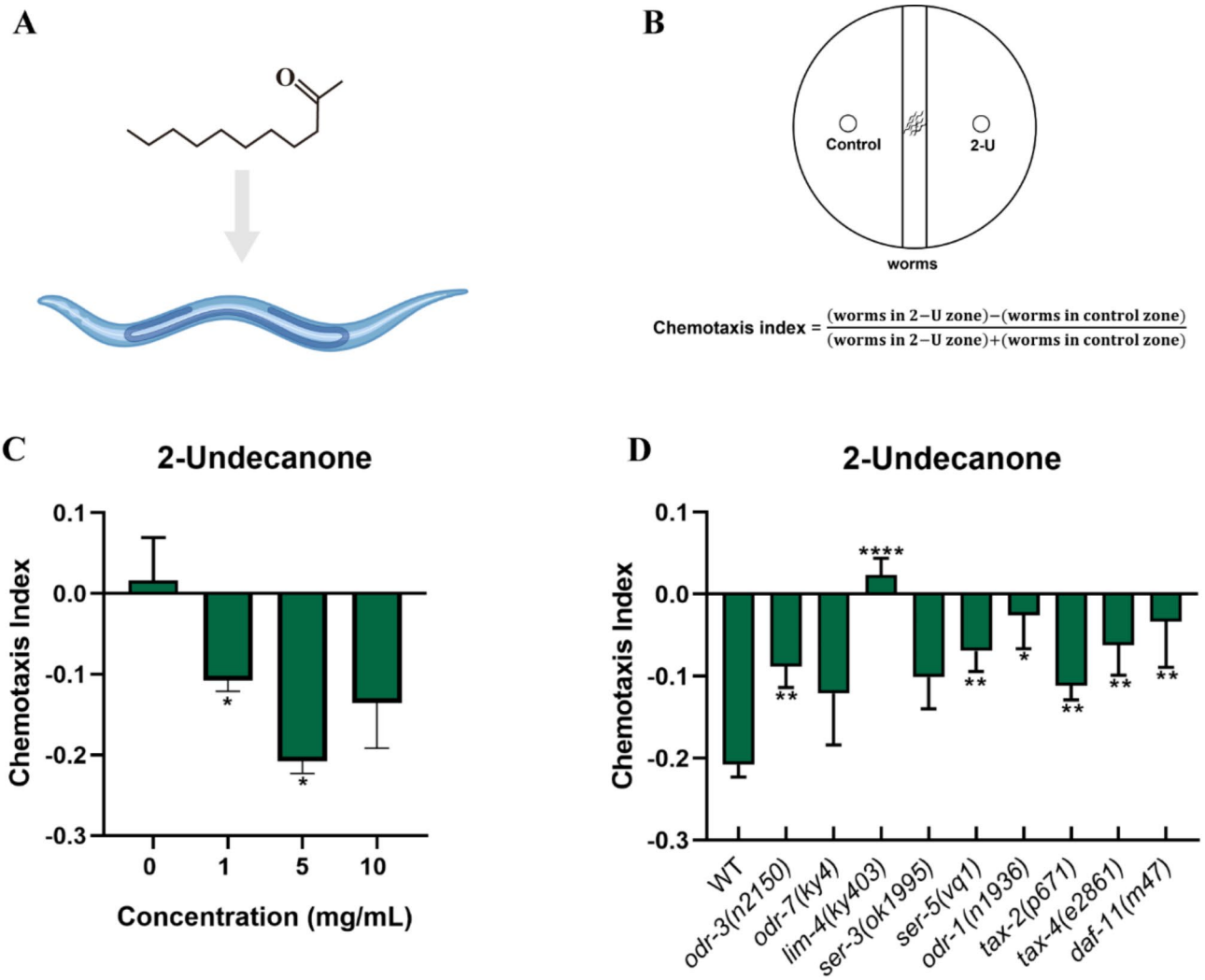

Fig. 1. Chemotactic response of *C. elegans* to 2-undecanone. (**A**) Overview of the 2-undecanone structural formula and *C. elegans*. (**B**) Schematic diagram of the chemotaxis assay. (**C**) Chemotaxis effects of 2-U at various concentrations. (**D**) Chemotaxis effects of 2-U at 5 mg/mL on WT, *odr-3 (n2150)*, *odr-7 (ky4)*, *lim-4 (ky403)*, *ser-3 (ok1995)*, *ser-5 (vq1)*, *odr-1 (n1936)*, *tax-2 (p671)*, *tax-4 (e2861)*, *daf-11 (m47)* animals. $n \geq 6$ assays. Error bars indicate means ± SEM. *, $P < 0.05$; **, $P < 0.01$; ****, $P < 0.0001$; (two-tailed unpaired Student's *t* test was used for statistical comparisons of the WT to the mutants). Generated by Adobe Illustrator 2020 (version number 28.0.0, https://www.adobe.com/products/illustrator.html).

C. elegans. We utilized necrosis-associated mutants to assess sensitivity to 2-undecanone and employed qPCR to detect the expression of necrosis-associated genes. Compared with the wild type, mutants in *tra-3*, *itr-1*, *asp-3* and *asp-4* decreased the sensitivity of *C. elegans* to 2-undecanone (Fig. 2F). The results of qPCR indicated that the necrosis-related genes *itr-1*, *tra-3*, *asp-3*, and *asp-4* were significantly upregulated (Fig. 2G). Collectively, these data indicated that the traditional necrosis signaling pathway was involved in the reaction of *C. elegans* to 2-undecanone.

Lysosomes contain a variety of enzymes that can be released into the cytoplasm, causing severe necrosis and triggering apoptosis. We thus explored whether treatment with 2-undecanone leads to the release of crucial enzymes from the lysosome. We carried out time-lapse analyses to track the dynamic changes of GFP - fused Galectin 3. This protein has the ability to bind to the β-galactosides of glycoprotein hydrolases. When lysosomal membranes are ruptured, these hydrolases are released. Subsequently, GFP-fused Galectin 3 binding to the β-galactosides of the released hydrolases generates green fluorescence in the cytosol[27,28]. In 2-undecanone-treated worms expressing the m-Cherry-labeled luminal hydrolases CRP-6, GBA-3 and CPL-1, GFP-fused Gal 3 initially appeared around the lysosomes and then gradually enriched the area where mCherry fluorescence disappeared (Fig. S1). This result is consistent with the results of Lyso-Tracker staining and suggested that 2-undecanone damages lysosomal membranes, leading to the release of CPR-6, GBA-3, CPL-1 into the cytosol. Once there, these hydrolytic enzymes aggravate necrosis and eventually lead to the death of *C. elegans.*

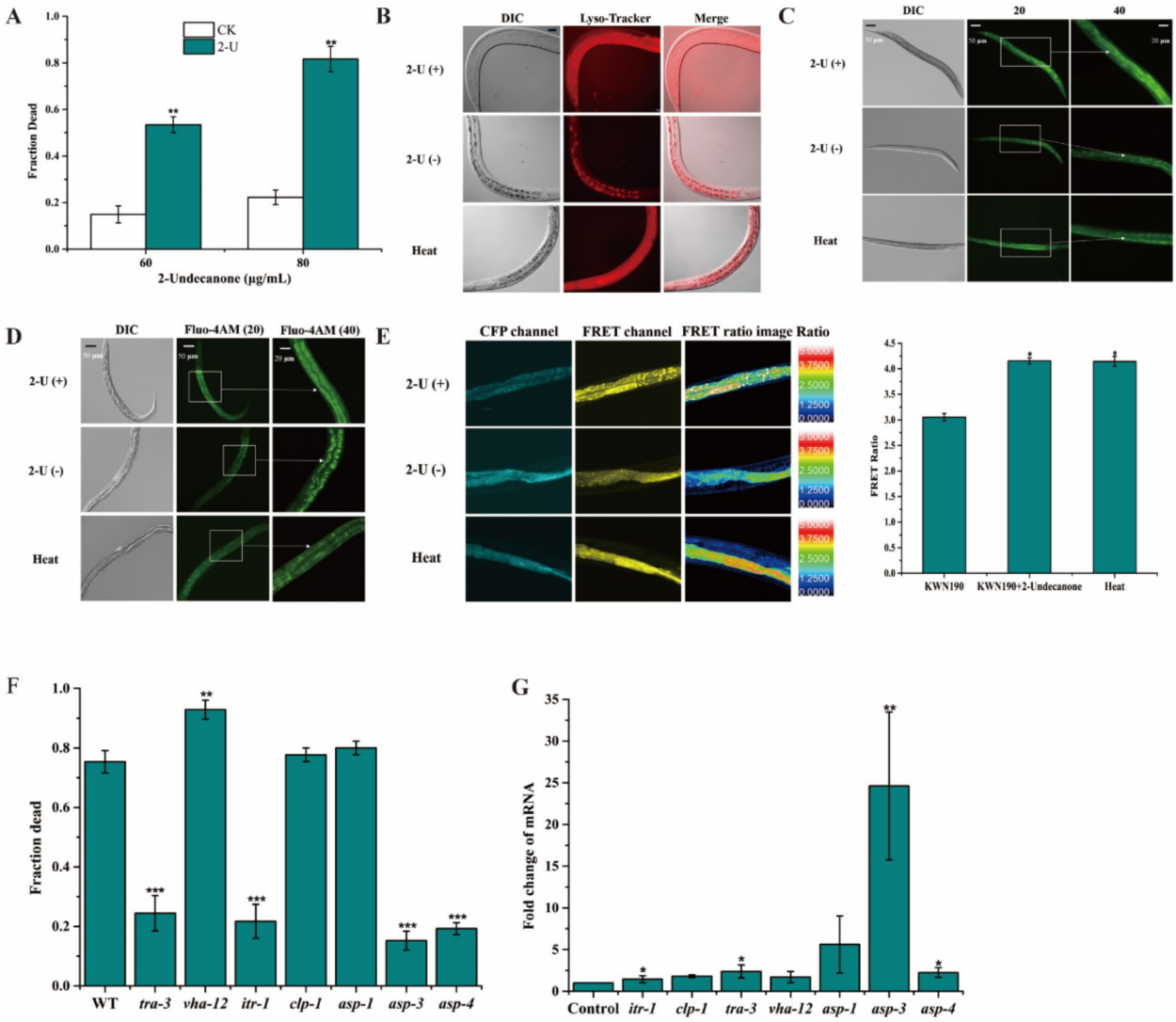

Fig. 2. 2-Undecanone induces necrosis in *C. elegans* cells. (**A**) Nematocidal activity of 2-undecanone on *C. elegans* after 48 h. (**B**) *C. elegans* stained intestinal lysosomal marker Lyso-tracker in vitro. (**C**) Observation of the lysosome of *C. elegans* pwIs50 in vivo. Heat stroke treatment is positive control. Scale bars, 20 μm. (**D**) *C. elegans* stained by calcium indicator Fluo-4AM in vitro. (**E**) In *C. elegans* KWN190 in vivo, right shows that the FRET ratio increased treatment with 2-undecanone or heat stroke (**F**) Nematocidal activity of 2-undecanone against mutants of necrosis pathway of *C. elegans*. Mortality of *tra-3(e2333)*, *itr-1 (sa73)*, *clp-1 (e907)*, *vha-12 (ok821)*, *asp-1 (tm666)*, *asp-3 (tm4559)* and *asp-4 (ok2693)* necrosis exposed to 2-undecanone. (**G**) Quantitative PCR (qPCR) analysis of *tra-3*, *itr-1*, *clp-1*, *vha-12*, *asp-1*, *asp-3* and *asp-4* necrosis-associated gene levels in 2-undecanone-treated *C. elegans* and control *C. elegans* for 3 h. Cell division control protein 42 homolog (*cdc-42*) served as an internal control. The bars represent means ± SD of three independent experiments. **P* < 0.05, ** *P* < 0.01, *** *P* < 0.001.

Hsp70 A and V-ATPase A are target proteins interacting with 2-undecanone in *C. elegans*

To further investigate the mechanism of cell death in *C. elegans* by 2-undecanone, we utilized drug affinity responsive target stability (DARTS), an unbiased biochemical approach based on the altered protease susceptibility of target proteins upon drug binding[29,30]. According to the results of SDS-PAGE, the bands at 70, 35 and 25 kDa (Fig. S2A) in the lysate from 2-undecanone treated *C. elegans* postproteolysis were more intense than those from the vehicle control. Mass spectrometry analysis of the three bands showed that the V-type proton ATPase catalytic subunit A (V-ATPase A), the heat shock 70 kDa protein A (Hsp70 A), along with several other proteins at 35 and 25 kDa, were enriched in the 2-undecanone-treated (Table S1). We therefore selected Hsp70 A and V-ATPase A for heterologous expression in *Escherichia coli* and purification, and got the tag-free proteins (Fig. S2 B-E) for further interaction analysis.

Interactions between the purified Hsp70 A or V-ATPase A and 2-undecanone were evaluated in vitro using microscale thermophoresis (MST, Monolith NT.115). Although the results of an initial capillary scan showed

nonspecific binding of the labeled Hsp70 A or V-ATPase A to the capillary walls (Fig. 3A and C), subsequent analyses of the MST curves revealed strong binding between these proteins and 2-undecanone. Specifically, the K_D values were determined to be 117.33 ± 16.26 nM for Hsp70 A and 301.67 ± 43.92 nM for V-ATPase A, respectively (Fig. 3B and D). These results are consistent with the hypothesis that Hsp70A and V-ATPase A are target proteins of 2-undecanone. We next employed RNAi to study the interaction between 2-undecanone and the two proteins in vivo. Our results showed that *hsp-1*, *vha-13* or *hsp-1*/*vha-13* RNAi worms treated with 2-undecanone had significantly lower mortality than did worms in the wild type control group (Fig. 3E). We also used LysoTracker red staining to ascertain whether 2-undecanone induced lysosome rupture in RNAi-treated worms to the same degree as it did in the wild type strain. We observed that before 2-undecanone treatment, the lysosomes of all the worms were normal and without obvious rupture, whereas after treatment, lysosomal membranes of the wild type worms were permeabilized as indicated by bursting of red fluorescence. In contrast, only slight lysosomal rupture was seen in the *hsp-1*, *vha-13* or *hsp-1*/*vha-13* RNAi worms (Fig. 3F), providing further substantiation for the idea that Hsp70 A and V-ATPase A are target proteins of 2-undecanone in *C. elegans*.

We extracted lysosomes of *C. elegans* (Fig. S3) to confirm the subcellular localization of the Hsp70 A and V-ATPase subunit A proteins. Western blots were used to determine whether the target proteins were present in the extracted lysosomes and to monitor changes in the lysosome proteins. We found higher levels of active acid phosphatase in lysosomal suspensions from the 2-undecanone-treated worms and *hsp-1(tm5076)* mutant worms than in those from unexposed worms or wild-type worms. This finding suggested that membrane integrity is influenced by 2-undecanone and is also affected in the lysosomes of *hsp-1(tm5076)* mutant worms. (Fig. S4). The Western blots also showed clearly that Hsp70 A and V-ATPase subunit A are located on lysosomes. Moreover, the expression of these proteins did not change significantly when treated with 2-undecanone (Fig. S5), laying the foundation for our subsequent investigation.

2-Undecanone impacts sphingomyelin metabolism in *C. elegans*

To further elucidate the molecular basis of lysosome rupture induced by 2-undecanone, we investigated whether 2-undecanone affected sphingomyelin metabolism in *C. elegans*. The results revealed a significant reduction in acid sphingomyelinase (ASM) activity following 2-undecanone treatment and in *hsp-1* mutant worms (Fig. 4A). The expression of *asm-1* and *asm-2*, which encode acid sphingomyelinase (ASM), but not that of *asm-3*, as well as the expression of *asah-1* and *asah-2*, which encode acid-ceramidase, were significantly reduced by 2-undecanone treatment. (Fig. 4B and C). We also tested whether the lysosomes of *asm* mutant worms were more sensitive to 2-undecanone than those of the wild type. Remarkably, the lysosomes of all the *asm* mutant

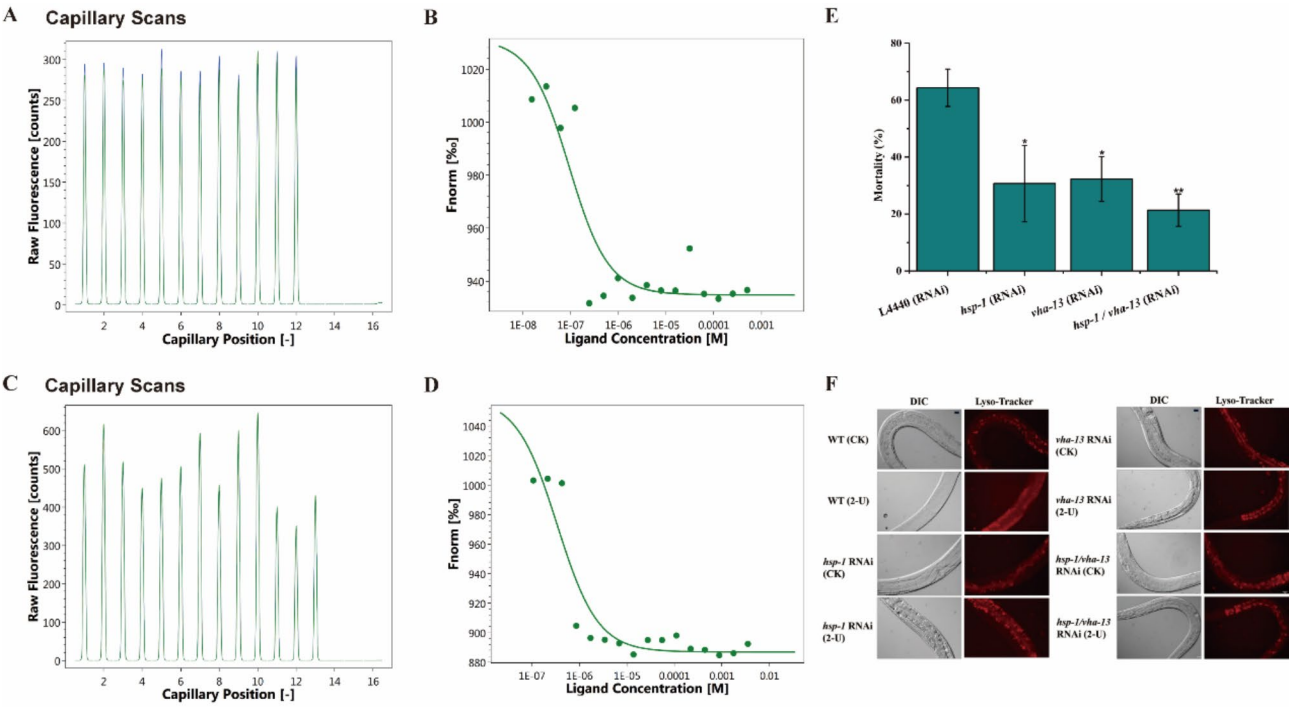

Fig. 3. Interactions between 2-undecanone and the target proteins Hsp70 A and V-ATPase A. (**A**) Fluorescence counts of Hsp70 A-RED protein. (**B**) Dose-response curve for the binding interaction between Hsp70 A and 2-undecanone by using MST analysis. (**C**) Fluorescence counts of V-ATPase-A-RED protein. (**D**) Dose-response curves for the binding interaction between V-ATPase-A and 2-undecanone by using MST analysis. (**E**) Sensitivity of *hsp-1*, *vha-13* or *hsp-1*/*vha-13* RNAi worms to 2-undecanone. Data represents means ± SD from triplicate experiments. *$P < 0.05$, ** $P < 0.01$ (**F**) *hsp-1*, *vha-13* or *hsp-1*/*vha-13* RNAi worms stained by intestinal lysosomal marker Lyso-Tracker. $N = 6$, scale bars, 20 μm.

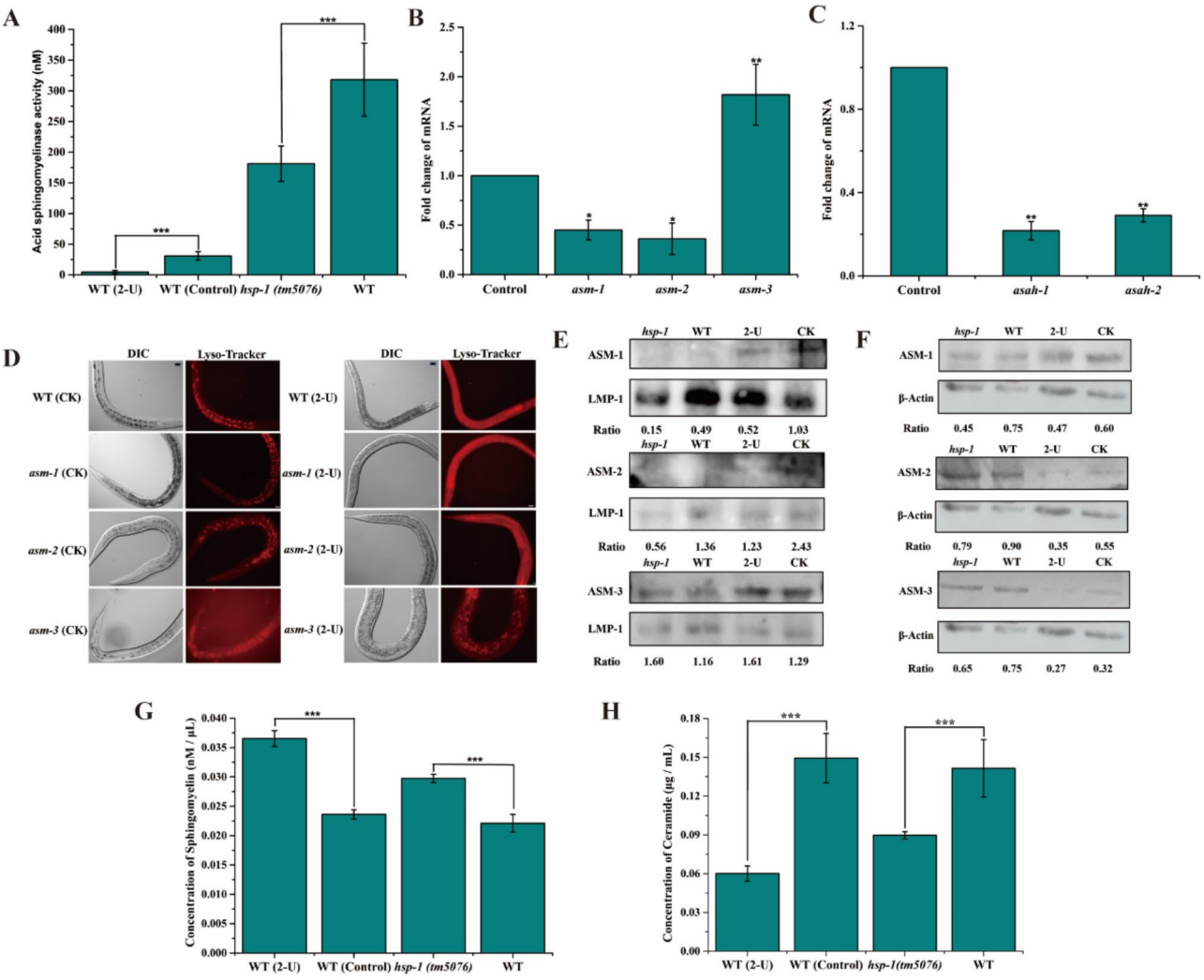

Fig. 4. 2-Undecanone alters sphingomyelin metabolism and destabilizes lysosomes. (**A**) Acid sphingomyelinase (ASM) activity in lysosomes. WT (2-U), lysosomes from 2-undecanone-treated worms. WT (Control), lysosomes from 2-undecanone-control worms. *hsp-1 (tm5076)*, lysosomes from non-treatment hsp-1 worms. WT, lysosomes from non-treatment worms. Quantitative PCR (qPCR) analysis of *asm-1*, *asm-2*, *asm-3* (**B**), *asah-1*, *asah-2* (**C**) genes levels in 2-undecanone-treated *C. elegans* and 2-undecanone-control *C. elegans* for 3 h. Cell division control protein 42 homolog (*cdc-42*) served as an internal control. (**D**) Sensitivity of lysosomes of *asm-1*, *asm-2*, *asm-3* mutants stained by intestinal lysosomal marker Lyso-Tracker to 2-undecanone. Scale bars, 20 μm. Expression levels of ASM-1, ASM-2 and ASM-3 of 2-undecanone-treated worms and *hsp-1* (*tm5076*) mutants in lysosomes with LMP-1 as an internal control (**E**). Total protein with β-Actin as an internal control (**F**). In total protein, β-Actin served as an internal control. (**G**) SM concentrations of lysosomes as measured by Sphingomyelin assay kit. (H) Ceramide concentration of lysosomes was measured based on HPLC- fluorescence detecting method. The data represents means ± SD from triplicate experiments. $^{*}P < 0.05$, $^{**}P < 0.01$, $^{***}P < 0.001$.

worms appeared undamaged prior to treatment with 2-undecanone, whereas after treatment, the lysosomal membranes of *asm-1* and *asm-2* mutant worms, but not *asm-3* mutant worms, were permeabilized (Fig. 4D). Next, to determine whether ASM is downregulated after treatment with 2-undecanone or in *hsp-1* mutant worms, we quantified ASM in whole protein and lysosome-enriched fractions of *C. elegans* by densitometric analysis of Western blots. In both treated worms and *hsp-1* mutants, we observed a significant decrease in the expression of ASM-1 and ASM-2 in both whole protein extracts and lysosome-enriched fractions. However, this reduction was not evident for ASM-3, with no significant changes observed in either treated or mutant worms compared to untreated controls and wild-type worms. (Fig. 4E and F). Based on these results, we speculated that *asm-1* and *asm-2* play an important role in maintaining the stability of *C. elegans* lysosomes.

The accumulation of sphingomyelin leads to lysosome destabilization[31], while low sphingomyelin levels may be critical to maintain the integrity of the lysosomal membrane[32]. Therefore, we quantified sphingomyelin levels, and found that they were increased after 2-undecanone treatment in the wild type and in *hsp-1* mutant

worms as compared with in untreated controls and wild-type worms (Fig. 4G). Moreover, the levels of lysosomal ceramide, a product of ASM activity, were measured by HPLC-fluorescence. The results showed that these levels were significantly decreased in both the wild-type worms after 2-undecanone treatment and in *hsp-1* mutants (Fig. 4H). Ceramide can affect the physical properties of the membrane, such as its fluidity, and promote the proper organization of lipids, thereby contributing to the stabilization of the lysosomal membrane[33]. Based on these results, we speculated that 2-undecanone first binds to the target protein Hsp70 A in the lysosomal membrane. As a result, it affects the stability of the lysosomal membrane by decreasing the activity of ASM, reducing the ceramide level, and increasing the sphingomyelin level.

Discussion

The annual loss caused by root-knot nematodes in global agricultural production amounts to as much as 70 billion US dollars[34–36]. Control of RKNs has become an eternal challenge in agricultural production[37]. Early studies have shown that the volatile metabolite 2-undecanone owns dual effects on nematodes, namely repellency and contact killing[6]. In this study, we use *C. elegans* as a model to understand the mechanism of the dual functions (repellency and nematocidal toxicity) of 2-undecanone. 2-undecanone is a volatile compound produced by the bacterial strain *Paenibacillus polymyxa* KM2501-1, which has the ability to protect plants against pathogenic nematodes. We show that olfaction-mediated modulation of behavior by 2-undecanone is dependent on neuronal signaling in AWB odor sensory neurons. Then, the signal is transduced via the cGMP pathway to trigger the repellent behavior.

The volatile metabolite 2-undecanone belongs to a category of methyl ketones, which are broadly distributed in natural environments and can be produced by various organisms. This category of substances also includes 2-heptanone, produced by the bacterium *Bacillus nematocida* B16. This compound has been shown to elicit an attraction response in *C. elegans* by binding to the GPCR receptor STR-2, which is expressed in AWC neurons[24]. The volatile substance styrene, produced by *Bacillus mycoides* strain R2 and recognized through the AWB neurons of nematodes, also has a chemotaxis effect on nematodes[38]. These indicate that methyl ketones have certain effects on nematodes prevention and control. Much research has been done on their mechanisms, yet the targets or signaling pathways of these substances vary. Few of these substances displayed dual functions against nematodes, and even fewer studies have been carried out on the mechanisms underlying these dual functions.

We identified Hsp70 A and V-ATPase A as the targets of 2-undecanone in *C. elegans*. The binding of 2-undecanone to these targets led to an increase in intracellular calcium levels and the rupture of the lysosomal membrane in *C. elegans*, which induced necrosis and ultimately caused cell death.

Lysosomal membrane permeabilization plays a crucial physiological role, as it can lead to the abnormal activation of hydrolases, including caspases. This can result in membrane trafficking defects, disrupted energy metabolism, and ultimately cell death through necrosis or apoptosis[14,15]. Lysosome-associated membrane proteins (LAMPs) are the most plentiful glycoproteins in the lysosome membrane, which is thought to protection role against lysosomal hydrolases[39]. However, in *C. elegans*, deletion of LMP-1 and LMP-2, the homologues of important human LAMP proteins, did not cause severe damage to lysosome membranes. This finding suggests that the loss of LMPs has only a slight impact on lysosomal function[19]. Instead, we found that 2-undecanone bound to and down-regulated expression of Hsp70 A, decreasing acid sphingomyelinase (ASM) activity, increasing the level of sphingomyelin, decreasing the level of the ASM product ceramide and finally resulting in lysosomal rupture and death. We observed similar results with *hsp-1* mutants, clearly indicating that Hsp70 A has a key role in maintaining lysosomal stability. Moreover, since ASM inhibition and the subsequent sphingomyelin accumulation are key changes in sphingolipid metabolism that underlie the nematocidal effect of 2-undecanone, it is not surprising that ASM also plays an important role in protecting nematode viability. Indeed, the lysosomes of *asm* mutants were more sensitive to 2-undecanone than those of the wild-type. This is consistent with the theory that 2-undecanone acting on Hsp70 A, it triggers a cascade of reactions, leading to reduced acid sphingomyelinase activity.

Both the V-ATPase A and Hsp70 A proteins have been implicated in nematode viability. For example, Coboni et al. found previously that the butyrolactone tulipaline A exhibited strong nematocidal activity against *M. incognit*a and *M. arenaria*. Like bafilomycin A1, B1, C1 or D, which are vacuolar-type H+-ATPase (V-ATPase) inhibitors, tulipaline A caused paralysis or death in the nematodes, suggesting that the toxic effects of lactones and aldehydes might be a consequence of their inhibition of V-ATPase[35]. Knockdown of V-ATPase A produced a striking protein-aggregation phenotype in oocytes from hermaphrodites[40]. Moreover, overexpression of *mec-4 (d)* (a calcium-conducting ion channel subunit of V-ATPase) in mechanosensory neurons of *C. elegans* caused neurodegenerative cell necrosis. In studies on the V-ATPase mutants *spe-5*, *unc-32*, and *vha-12*, interference with the genes *vha-2*, *vha-10*, and *vha-12* or when bafilomycin A1 or filomycin was added, the cell necrosis caused by mec-4 (d) was inhibited. Collectively, these results supported the necessity of V-ATPase activity for the execution of necrosis[41]. In other studies, Kirkegaard et al. found that Hsp70 can stabilize lysosomes by binding to an endolysosomal anionic phospholipid, bis (monoacylglycero) phosphate[33]. Petersen et al. found that antineoplastic drug siramesine inhibits ASM by interfering with its activity through binding with (bis (monoacylglycero) phosphate)[42]. Yamashima et al. provided a modified "calpain–cathepsin hypothesis" proposing that activated calpain cleaves oxidative stress–induced carbonylated Hsp70.1, resulting in lysosomal rupture[43]. Oxidative stress-induced Hsp70.1 carbonylation, synergistic with calpain-mediated cleavage, led to lysosomal rupture, release of cathepsin, and neuronal death[44]. Regarding the V-ATPase, in *C. elegans*, V-ATPase is a multi-subunit complex organized into two functional domains. In the V1 domain, there are eight different subunits, designated A to H, the Vo domain is composed of five different subunits: a, c, c`, d and e[45]. The gene *vha-13* encodes ATP synthase, which is expressed in the intestine, body wall muscles and excretory canals. RNAi of *vha-13* resulted in embryonic lethality, growth defects and sterility[46]. So, these two proteins are essential for life of cell and organisms.

In summary, our study proposes a model of the repel – kill action of 2-undecanone on *C. elegans* (Fig. 5A). When the concentration of 2-undecanone reaches a high level (1–5 mg/mL), the AWB neurons of the nematode perceive the odorant and transduce the signal through the cGMP pathway, leading to the completion of avoidance behavior by the nematode (Fig. 5B). At lower concentrations of 2-undecanone (0.06–0.08 mg/mL), 2-undecanone induces an increase in concentration of the intracellular calcium, lysosomal membrane rupture, and triggering the necrosis pathway in *C. elegans* (Fig. 5C). We have also shown that 2-undecanone interacts with Hsp70 A to decrease ASM activity, increase the level of sphingomyelin, and reduce ceramide levels. These changes then induce lysosomal rupture and cell necrosis. Although our study revealed some important findings, there are still many questions that remain for future investigation. Firstly, the entire signaling pathway by which Hsp70 A is involved in maintaining lysosomal integrity remains unknown. The potential roles of several factors remain to be determined in this context. These factors include bis(monoacylglycero)phosphate[33], oxidative stress-induced carbonylation of Hsp70.1. This carbonylation has been observed in other system to lead to lysosomal destabilization and the release of cathepsins[32]. Additionally, there is calpain activation, which is accompanied by a concomitant decrease in the lysosomal membrane localization of Hsp70.1 and BMP levels[18]. V-ATPase A is also a target of 2-undecanone, but its potential effect on the acidification function of V-ATPase A remains to be investigated.

The contact-toxicity targets of 2-undecanone against the nematode are Hsp70 A and V-ATPase. Multiple targets can inhibit the nematode's tolerance to the insecticidal substance. While other studies have shown that single functional substances for nematode control have been identified to bind to multiple targets[3,11]. Prolonged use of chemical substances can lead to the development of resistance. The dual functions and multi-targets of 2-undecanone have the potential to reduce nematode tolerance to the compound and facilitate the development of novel strategies for nematode control.

Materials and methods

C. elegans

Strains of *C. elegans* were cultured and maintained at 20 ℃ on nematode growth medium plates[47]. The N2 Bristol strain was used as the wild type. The *Caenorhabditis* Genetics Center (CGC) provided the following strains used in the genetic analyses: *asp-1 (tm666)*, *asp-3 (tm4559)*, *asp-4 (ok2693)*, *odr-1 (n1936)*, *odr-3 (n2150)*, *odr-*

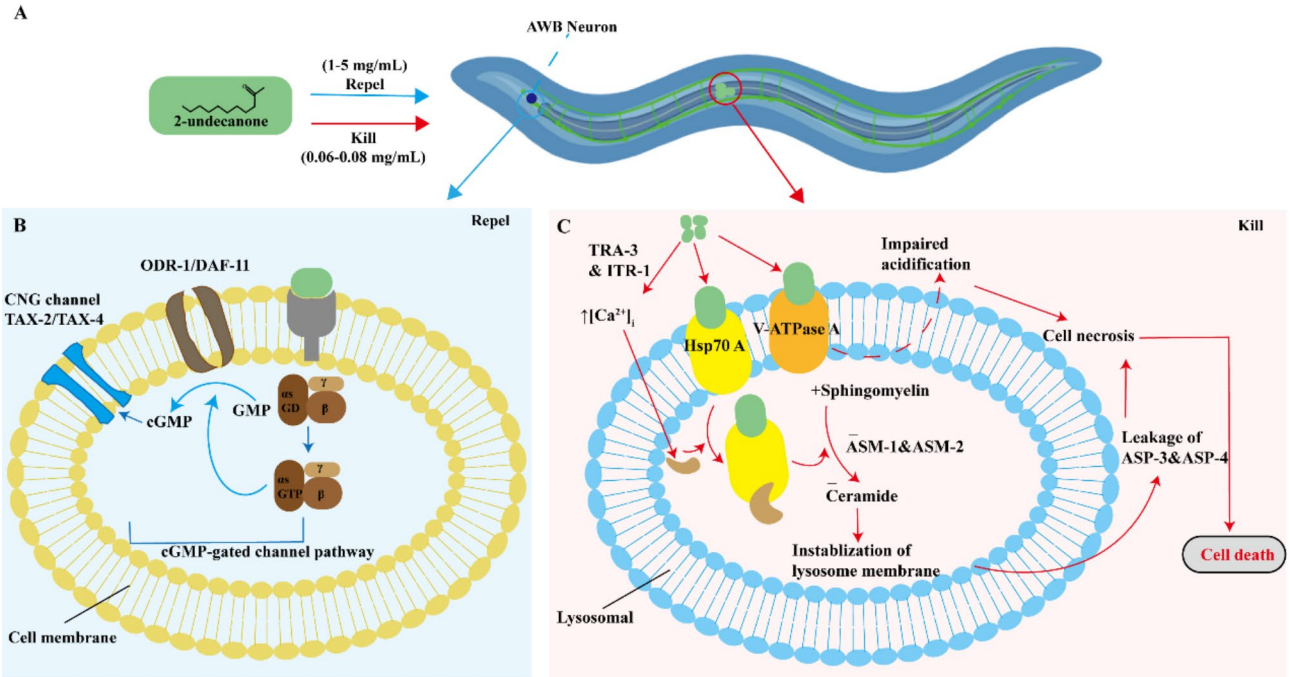

Fig. 5. Molecular model of the dual function of 2-undecanone on *C. elegans*. (**A**) A model of the repel-and-kill effect of 2-undecanone on *C. elegans*. 2-Undecanone emits expelled odors which is detected by the AWB olfactory of *C. elegans*. (**B**) Molecular mechanism of the repellent response of *C. elegans* induced by 2-undecanone. Nematodes sense 2-undecanone signal that is dependent on neuronal signaling in AWB odor sensory neurons. Then, the signal is transduced via cGMP pathway. (**C**) Molecular mechanism of 2-undecanone killing *C. elegans*. 2-Undecanone first binds to the target protein Hsp70 A, and inhibits ASM activity, leading to the accumulation of SM. This results in increased membrane permeability of the lysosome and the release of cathepsin from the lysosome into the cytoplasm, triggering cell death. In addition, 2-undecanone can also bind to V-ATPase A, impairing the acidification inside lysosomes and exacerbating the cell death process of lysosomes. Generated by Adobe Illustrator 2020 (version number 28.0.0, https://www.adobe.com/products/illustrator.html).

7 (ky4), *lim-4 (ky403)*, *ser-3 (ok1995)*, *ser-5 (vq1)*, *tax-2 (p671)*, *tax-4 (e2861)*, *daf-11 (m47)*, *itr-1 (sa73)*, *clp-1 (e907)*, *tra-3 (e2333)*, *vha-12 (ok821)*, *rrf-3 (pk1426)*, pwIs50[lmp-1 :: GFP + Cbr-unc-119(+)], and rnyEx109 [nhx-2p::D3cpv + pha-1 (+)]. The *asm-1(tm5267)*, *asm-2(tm3746)*, *asm-3(tm2384) and hsp-1(tm5076) constructs* were obtained from the Japan National Bioresource Project. The RnyEx109 strain carries an integrated transgene that enables the expression of the calcium indicator d3cpv, regulated by the intestine-limited promoter Pnhx-2 [47,48]. Integrated transgene strain PwIs50 expressed the intestinal lysosomal marker LMP-1::GFP[49,50].

We obtained *qxIs257* (P*ced-1*NUC-1:: mCherry), *qxIs352* (P*ced-1*LAAT-1:: mCherry), *qxIs594* (P_{myo-3}sfGFP::Gal3), *kxEx147* (P_{gba-3}GBA-3::mCherry), *yqEx632* (P*cpl-1*CPL-1::mCherry), and *kxEx141* (P_{cpr-6}CPR-6::mCherry) from Xiaochen Wang (Chinese Academy of Sciences, Beijing, China).

Nematicidal activity of 2-undecanone against *C. elegans*

C. elegans were cultured with *Escherichia coli* OP50. Synchronized worms were obtained by treating with 5% sodium hypochlorite: 5 M sodium hydroxide (2:1, *v / v*), followed by embryo hatching on NGM plates fed with a little OP50. After overnight incubation for hatching, synchronized worms were L1 larvae. Approximately 12 h feeding, worms were L2 larvae. Synchronized L2 worms were tested for nematicidal activity of 2-undecanone.

Chemotaxis index of 2-undecanone against *C. elegans*

Petri plates containing10 mL of 2% sterilized water agar with a diameter of 90 mm were carefully prepared. The area 8 mm wide surrounding the central line of the plate serves as a buffer zone, with the left side being the control area and the right side being the experimental (2-undecanone) area. Sterilized filter paper discs (diameter 8 mm) are placed at the center points of both the control and experimental areas. Then, 30 µL of 2-undecanone solution at different concentrations (dissolved in anhydrous ethanol) is placed on the filter paper discs in the experimental zone, while the same volume of anhydrous ethanol is placed on the filter paper discs in the control zone. L2 *C. elegans* are placed in the center area of the plate, with a maximum of 150 nematodes in each plate. After incubation in the dark at 20℃ for 2 h, the count of nematodes in both the experimental and control zones were conducted using an inverted microscope, excluding those in the buffer region.

LysoTracker red staining, acridine orange staining and calcium imaging

Lyso-Tracker Red (Beyotime, China) was used in vitro to evaluate lysosomal membrane integrity in *C. elegans*. L4 worms were soaked in 200 µL Lyso-Tracker Red in M9 buffer (Na_2HPO_4•$7H_2O$ 5.8 g, KH_2PO_4 3.0 g, NaCl 5.0 g, $MgSO_4$•$7H_2O$ 0.25 g, pH7.4) (1:13000) for 2 h at 20 ℃ in the dark. Worms were rinsed three times with M9 buffer before examination under a fluorescence microscope. The *C. elegans* transgenic strain (pwIs50) expressing the intestinal lysosomal marker LMP-1::GFP was used to test lysosome integrity in-vivo. A solution with 2.5% pure ethanol served as the negative control, while exposure to 39℃ heat shock for 15 min acted as the positive control.

The calcium indicator Fluo-4 AM (Beyotime, China) was used i*n vitro* to monitor fluctuations in cytoplasmic calcium concentrations ($[Ca^{2+}]_i$) by assessing cytoplasmic fluorescence. L4 worms were soaked in 200 µL Fluo-4 AM in M9 (1:1000) for 1 h at 20℃ in the dark. Worms were then washed three times in M9 buffer and incubated for another 30 min to ensure complete transformation of Fluo-4 AM to Fluo-4 before examination by fluorescence microscopy. Calcium levels i*n vivo* were visualized by using the calcium indicator d3cpv expressed from the specific intestine promoter Pnhx-2 in transgenic strain rnyEx109 of nematodes. A solution with 2.5% pure ethanol served as the negative control, while exposure to 39℃ heat shock for 15 min acted as the positive control.

Drug affinity responsive target stability

Wild-type *C. elegans* of various ages were grown on NGM/OP50 plates, washed three times with M9 buffer solution, and immediately placed in the −80 ℃ freezer. The animals were lysed in HEPES buffer (40 mM HEPES pH 8.0, 120 mM NaCl, 10% glycerol, 0.5% Triton X-100, 10 mM β-glycerophosphate, 50 mM NaF, 0.2 mM Na_3VO_4, and protease inhibitors (Abmole, China)) using Lysing Matrix C tubes (MP Biomedicals, USA) and the FastPrep-24 (MP Biomedicals, USA) high-speed bench top homogenizer in a 4℃ room (disrupt for 20 s at 6.5 m/ s, rest on ice for 1 min; repeat twice). Lysed animals were centrifuged at 14,000 rpm for 10 min at 4 ℃ to pellet worm debris, and the supernatant was collected for DARTS. A worm lysate concentration of 2.54 µg/µL was used for the DARTS experiment. All steps were performed on ice or at 4℃. TNC buffer (50 mM Tris-HCl, 50 mM NaCl, 10 mM $CaCl_2$, pH 8.0) was added to the worm lysates. Worm lysates were incubated with a vehicle control (DMSO) or 2-undecanone for 1 h on ice and then 50 min at room temperature. Pronase (Yuanye, China) digestions were performed for 30 min at room temperature and stopped by adding SDS loading buffer and heating at 100 ℃ for 5 min. The resulting mixtures were separated by SDS-PAGE and stained with Coomassie Blue[51].

Gel lanes showing significant differences in intensity in the different samples were excised manually and subjected to an in-gel digestion procedure. Peptides were analyzed by high-resolution LC-MS/MS with an Eksigentnano-LC 415 System and Triple TOF 5600 (Applied Biosystem, USA). Mass spectra were acquired in a m/z range from 350 to 1250, and MS/MS spectra in a m/z range from 100 to 1800.

Protein expression and purification of Hsp 70 A and V-ATPase A

The Hsp 70 A and ATPase A full-length coding genes were synthesized and provided by the TsingKe company. The two gene sequences are from the NCBI database, and their accession number are NM070667 and NM074158. Standard methods of cloning, sequencing, and PCR amplification were used. Briefly, full-length *hsp-1* and *vha-13* were subcloned into the vector pMD18-T (Takara Bio Inc. China). Then the plasmids were extracted, digested with *EcoRI* and *SalI*, and cloned into pET32a[52] and pE-Sumo[53] to create the recombinant vectors pET32a-*hsp-1*

and pE-Sumo-*vha-13*. Transformed recombinant plasmids into *E. coli* BL21(DE3) and positive transformants were screened on LB plates with 100 μg/mL ampicillin added. Hsp 70 A and V-ATPase A were expressed in *E. coli* as the His-tagged fusion proteins Hsp 70 A –Trx and V-ATPase A-Sumo, respectively, then purified by Ni-NTA. Finally, the Trx and Sumo tags of the purified recombinant proteins were removed by enterokinase (rEK) (Solarbio, China) (1:500 (U/μg)) and Ulp (Solarbio, China) (1:100 (U/μg)), respectively, yielding the tag-free proteins Hsp 70 A and V-ATPase A.

Binding measurement by MST in vitro and RNAi in vivo

The tag-free proteins Hsp 70 A and V-ATPase A were diluted to 12 μM after concentrated by ultrafiltration. Then proteins were labeled using RED-NHS 2nd generation depending on the user's manual for Monolith NT.115 (Nano Temper, Germany). Labeled protein samples were diluted with a buffer solution containing 20 mM Tris-HCl and 300 mM NaCl at a pH of 8.0 to ensure that the fluorescence values remained within the range of 200 to 1500. The 2-undecanone was dissolved in DMSO, and 12 kinds of concentrations were obtained through dilution steps. First, mix the 12 samples with the labeled protein in equal parts. Then, fill the capillaries in MST kit with the resulting mixture and place them on a tray to prepare for measuring the binding affinity. According to the binding curve, the K_D values were calculated[39,54].

For the RNAi experiments, the bacterium-feeding protocol was as described before[55]. In the *hsp-1* and *vha-13* RNAi experiments, 1000 L1 larvae of *C. elegans* were cultured on the RNAi plates and sensitivity of RNAi *C. elegans* to 2-undecanone and lysosome damage was examined.

Microscopy and imaging analysis

For lysosome integrity observations, nematodes were placed on a glass slide and differential interference contrast and fluorescence images were captured with an Olympus BX63 microscope at 400 magnifications. Images were processed and viewed using Olympus cellSens imaging software.

For calcium imaging observation in vitro, nematodes were placed on a glass slide and differential interference contrast and fluorescence images were captured with an Olympus BX63 microscope at 400 magnifications. The excitation and emission wavelengths were 489 nm and 508 nm, respectively. The relative fluorescence (F1/F0) was calculated using computerized image analysis with Olympus cellSens imaging software, where F1 was the fluorescence of *C. elegans* exposed to 70 μg/mL 2-undecanone for 2 h or heat shock, and F0 was the fluorescence of *C. elegans* without 2-undecanone or heat shock[56]. Calcium levels in vivo were visualized using the calcium indicator d3cpv expressed from the intestine-limited promoter Pnhx-2 in transgenic (rnyEx109) nematodes. Nematodes were imaged under an Olympus FV1000 inverted confocal IX81 microscope. CFP (405 excitation, 480 emission), and FRET (405 excitation, 535 emission) filters and FV10-ASW software were used to collect the FRET data. The FRET ratio was calculated by $(FRET_{int}–FRET_{bkgnd)}/(CFP_{int}–CFP_{bkgnd})$, where $FRET_{int}$ and CFP_{int} represent the fluorescent intensities of the FRET and CFP channels of nematode the gut, and $FRET_{bkgnd}$ and CFP_{bkgnd} are the fluorescent intensities of FRET and CFP in the background region[57].

Confocal laser scanning microscopy

L4 larvae were exposed to 60 μg/mL 2-undecanone and then promptly subjected to 5 mM levamisole, a treatment that immobilizes worms without impacting the hypodermis layer. Images of fluorescence were obtained using a 100× objective lens with type NF immersion oil on an inverted fluorescence microscope (fv1000mp, Olympus). For EGFP fluorescence, the excitation and emission wavelengths were 488 nm and 507 nm, respectively. For mCherry fluorescence, the excitation and emission wavelengths were 580 nm and 610 nm, respectively. To test dynamic alterations in worms co-expressing sfGFP: Gal3 and mCherry-tagged version of GBA-3, CPL-1, or CPR-6, photographs were captured per 1 min for 20 min.

Purification of lysosome and assessment of acid phosphatase activity

Lysosomes were purified from L4 larvae with lysosomal isolation kit (Sigma-Aldrich)[57]. Briefly, the lysosomal fraction was refined through a density gradient, which was established using Optiprep and sucrose in increasing concentrations (from bottom up: 27, 19, 16 and 8% *w/v*). After centrifugation, the lysosomes enrichment in various fractions (from bottom to top: B1-4) was quantified, and after standardization to the same total protein concentration, lysosomal membrane proteins were examined using anti-LMP-1 antibody. The purified lysosomal fractions (B2 or B3) from wild-type and *hsp-1* mutant nematodes were standardized to same total protein concentrations and suspended in the extraction buffer provided in the kit. The activity of acid phosphatase present in the lysosomal suspension was determined utilizing acid phosphatase kit (CS0740; Sigma-Aldrich). The sample was incubated at 25 °C for 30 min, the reaction was stopped by addition of 0.5 M NaOH, and then the absorbance at 405 nm was measured. For each strain, three replicate experiments were conducted, and the average percentage of total activity was subsequently calculated[19].

Levels of acid sphingomyelinase (ASM), sphingomyelin and ceramide in lysosomes of *C. elegans*

The cytoplasmic lysate or lysosomal ASM activity was measured by high-performance liquid chromatography (HPLC) based on a fluorescent substrate as described previously[58,59]. First, a standard curve was made by assaying the peak area corresponding to different concentrations of BODIPY-C12 Ceramide (25997; Cayman, Canada). The standard 6 μL ASM assay mixture consisted of 3 μL of the cytoplasmic lysate or extracted lysosomes and 3 μL of assay buffer (100 μM BODIPY™ FL C12-sphingomyelin (ThermoFisher SCIENTIFIC; China), 0.2 mM $ZnCl_2$, 0.2% Lgepal CA-630, 0.2 M sodium acetate, pH = 5.0). Assays were carried out at 25 °C for 2 h. After the reactions were completed, 5 μL of the assay mixture was pipetted into 95 μL ethanol and centrifuged at 12,000 g for 5 min. The supernatant was transferred to a sampling vial and 10 μL was tested by HPLC which equipped

with an TC-C18 analytical column. The eluent was monitored with a fluorescence detector set to excitation and emission wavelengths of 505 nm and 540 nm, respectively. The peak of the product, B12Cer, was identified by comparing its retention time, and the amount of product was calculated using a regression equation which was established from the B12Cer standard curve.

The sphingomyelin quantification assay was carried out by using a sphingomyelin assay kit (MAK262; Sigma-Aldrich). In brief, 5 µL of the 5 mM SM standard was diluted with 245 µL of SM assay buffer to prepare a 100 µM standard solution. 0, 10, 20, 30, 40, and 50 µL aliquots of the diluted SM standard solution were added to a 96 well plate and SM assay buffer was added to each well to bring the volume to 50 µL. In addition, 2–10 µL of the cytoplasmic or lysosomal sample was added to the wells of a 96 well plate and the samples were brought to a final volume of 50 µL with SM assay buffer. Then 50 µL of the master reaction mix was added to each sample or standard control well. The plate was incubated for 1 h at 25 °C and absorbance was measured at 570 nm (A_{570}). The standard curve was plotted by using the corrected SM standard values after subtracting the blank value. The amount of sphingomyelin in the sample was calculated from the standard curve and the corrected sample readings. The concentration of sphingomyelin in the sample was then calculated as follows: $C = S_a/S_v$ (S_a is amount of sphingomyelin in the sample (nmole) from the standard curve, S_V is sample volume (µL) added to the wells. C is concentration of sphingomyelin in the sample).

The amount of ceramide in *C. elegans* was measured based on a HPLC–FLD method as described previously[59]. In brief, the standard curve was made by using the peak areas corresponding to different concentrations of N-acetyl-D-sphingosine (A7191; Sigma-Aldrich, China). Equal volumes of purified lysosomes were mixed with acetonitrile and centrifuged at 13,000 rpm for 3 min. The supernatant was added to 500 µL 1 M KOH ethanol solution to be deacetylated in a boiling water bath for 2 h, then reacted with derivatizing reagent o-phthalaldehyde for 60–90 s with a sample size of 50 µL. The analysis was performed with a TC-C18 column and methanol:0.02 M potassium dihydrogen phosphate solution (90:10, *v/v)* as the mobile phase at a flow rate of 1.0 mL/min. The excitation and emission wavelengths were set at 340 nm and 455 nm, respectively. The amount of ceramide in *C. elegans* was measured according to its peak area from the standard curve.

Western blotting analysis

The cytoplasmic lysate and lysosomes were separated by electrophoresis run on a 10% SDS-PAGE gel, transferred to nitrocellulose, and stained with Ponceau S. The membranes were incubated at room temperature with 5% (*w/v*) nonfat dry milk for 1 h in TBST buffer containing 20 mM Tris-HCl, 150 mM NaCl, 0.05% (v/v) Tween 20 and incubated overnight at 4 °C with the following primary antibodies: anti-Hsp 70 A at a dilution of 1:1000 (Boster Biological Technology, China); anti-V-ATPase A at a dilution of 1:1000; anti-Asm-1 at a dilution of 1:1000; anti-Asm-2 at a dilution of 1:1000; anti-Asm-3 at a dilution of 1:1000; anti-LMP-1 at a concentration of 0.4 µg/mL (DSHB, USA); and anti-β-actin at a dilution of 1:1000 (Beyotime). Membranes were washed before incubation with a horseradish peroxidase–conjugated antibody. BeyoECL and chemiluminescence (Beyotime, China) was used to visualize bands according to the manufacturer's instructions.

RNA isolation, reverse transcription and realtime PCR

Total RNA was isolated using the RNAsimple Total RNA Kit (TIANGEN) according to the manufacturer's instructions.

Realtime PCR was performed in 10 µL reactions with 0.2 µM final primer concentrations according to the kit protocols of BeyoFast™ SYBR Green qPCR Mix (2X, Low ROX) (Beyotime, China). Cycling conditions as follows were used to analyze the melting curve and to measure the specificity in each reaction tube: 50 °C for 2 min, initial denaturation at 95 °C for 2 min, followed by 40 cycles of 15 s at 95 °C, 30 s at 60 °C, and then 15 s at 95 °C, 15 s at 60 °C, and 15 s at 95 °C. The △△Ct method was used to calculate mRNA levels. The primers used are shown in Table 1.

Statistical analysis

The mortality rates of *C. elegans* in all assays were corrected by Abbott's formula. Data from all assays were analyzed by one-way analysis of variance with SPSS 20 (IBM, Armonk, NY, USA). The cutoff level for statistical significance was set to 5%, and all groups of data were tested for the comparability of their variances using an F test.

Gene	Primer	Amplicon size
itr-1 - Forward	5'- TTCGGAGTTGAGTGATAGC – 3'	171
itr-1 - Reverse	5'- ATCGTGTCTTCTGCCATC – 3'	
clp-1 - Forward	5'- ACAATGGTGGAGGTGGAA – 3'	105
clp-1 - Reverse	5'- CAACGCCGAGGAATCTG – 3'	
tra-3 - Forward	5'- CCAATTCTGACAGTGATGAC – 3'	177
tra-3 - Reverse	5'- GTGCTCCGCTCTTCTTG – 3'	
vha-12 - Forward	5'- GGAGAAGAAGCCTTGTCAT – 3'	140
vha-12 - Reverse	5'- ATACGGAGAAGTTGCCATC – 3'	
asp-3 - Forward	5'- GCCAACGACATCACCAA – 3'	111
asp-3 - Reverse	5'- GATTCTCCAGTAGTCCTCAG – 3'	
asp-4 - Forward	5'- CATACAAGGAGGATGGTAGAA – 3'	136
asp-4 - Reverse	5'- GGTTCACTGGTTGCTTCA – 3'	
cdc-42 - Forward	5'- CTGCTGGACAGGAAGATTACG – 3'	111
cdc-42 - Reverse	5'- CTCGGACATTCTCGAATGAAG – 3'	
asm-1 - Forward	5'- GTTGGATATGCTTCACCTTC – 3'	121
asm-1 - Reverse	5'- AATCGGCGTAATAAGTTGTG – 3'	
asm-2 - Forward	5'- CCGAAGACCATTCCACTT – 3'	127
asm-2 - Reverse	5'- CGCATCCTTGACCGTATA – 3'	
asm-3 - Forward	5'- GCTCTTGAAGGATATGCTCTA – 3'	161
asm-3 - Reverse	5'- GCCGAGTAGACCACATTAG – 3'	
asah-1 - Forward	5'- CTTGTCGGAGGATACTACG – 3'	155
asah-1 - Reverse	5'- ACTGGTGAGAGCATTGGA – 3'	
asah-2 - Forward	5'- TTCTCCTGGTTACGCTACT – 3'	159
asah-2 - Reverse	5'- GCTGACGAGGTGGAAGA – 3'	

Table 1. Primers used for realtime PCR.

Data availability

The datasets generated and/or analysed during the current study are available in the NCBI, ACCESSION NUMBER (NM070667 and NM074158).

Received: 30 December 2024; Accepted: 20 March 2025
Published online: 23 April 2025

References

1. Afridi, M. S. et al. Harnessing root exudates for plant Microbiome engineering and stress resistance in plants. *Microbiol. Res.* **279**, 127564 (2024).
2. La, S. et al. Protective role of native root-associated bacterial consortium against root-knot nematode infection in susceptible plants. *Nat. Commun.* **15** (1), 6723 (2024).
3. Niu, Q. et al. Q. A Trojan horse mechanism of bacterial pathogenesis against nematodes. *Proc. Natl. Acad. Sci. U.S.A.* **107** (38), 16631–16636 (2010).
4. Xie, J. et al. A novel *Meloidogyne incognita* effector Misp12 suppresses plant defense response at latter stages of nematode parasitism. *Front. Plant Sci.* **7**, 964 (2016).
5. Du, C. et al. Genetic and biochemical characterization of a gene operon for trans-Aconitic acid, a novel nematicide from *Bacillus Thuringiensis*. *J. Biol. Chem.* **292** (8), 3517–3530 (2017).
6. Cheng, W. et al. Volatile organic compounds from *Paenibacillus polymyxa* KM2501-1 control meloidogyne incognita by multiple strategies. *Sci. Rep.* **7** (1), 16213 (2017).
7. Huang, D. et al. Identification, characteristics and mechanism of 1-Deoxy-N-acetylglucosamine from deep-sea *Virgibacillus dokdonensis* MCCC 1A00493. *Mar. Drugs.* **16** (2), 52 (2018).
8. Zhang, Y., Lu, H. & Bargmann, C. I. Pathogenic bacteria induce aversive olfactory learning in *Caenorhabditis elegans*. *Nature* **438** (7065), 179–184 (2005).
9. Wan, X. et al. SRD-1 in AWA neurons is the receptor for female volatile sex pheromones in *C. elegans* males. *EMBO Rep.* **20** (3), e46288 (2019).
10. Prakash, D. et al. 1-Undecene from *Pseudomonas aeruginosa* is an olfactory signal for flight-or-fight response in *Caenorhabditis elegans*. *EMBO J.* **40** (13), e106938 (2021).
11. Cheng, W. et al. Multiple receptors contribute to the attractive response of *Caenorhabditis elegans* to pathogenic bacteria. *Microbiol. Spectr.* **11** (1), e0231922 (2023).
12. Ballabio, A. & Bonifacino, J. S. Lysosomes as dynamic regulators of cell and organismal homeostasis. *Nat. Rev. Mol. Cell Biol.* **21** (2), 101–118 (2020).
13. Mindell, J. A. Lysosomal acidification mechanisms. *Annu. Rev. Physiol.* **74**, 69–86 (2012).
14. Wang, F., Gómez-Sintes, R. & Boya, P. Lysosomal membrane permeabilization and cell death. *Traffic (Copenhagen Denmark)*. **19** (12), 918–931 (2018).
15. Repnik, U., Česen Hafner, M. & Turk, B. Lysosomal membrane permeabilization in cell death: Concepts and challenges. *Mitochondrion* **19** (Pt A), 49–57 (2014).
16. Oberle, C. et al. Lysosomal membrane permeabilization and cathepsin release is a Bax/Bak-dependent, amplifying event of apoptosis in fibroblasts and monocytes. *Cell Death Differ.* **17** (7), 1167–1178 (2010).

17. Dias, C. & Nylandsted, J. Plasma membrane integrity in health and disease: Significance and therapeutic potential. *Cell. Discov.* **7** (1), 4 (2021).
18. Zhu, H., Yoshimoto, T. & Yamashima, T. Heat shock protein 70.1 (Hsp70.1) affects neuronal cell fate by regulating lysosomal acid sphingomyelinase. *J. Biol. Chem.* **289** (40), 27432–27443 (2014).
19. Li, Y. et al. The lysosomal membrane protein SCAV-3 maintains lysosome integrity and adult longevity. *J. Cell Biol.* **215** (2), 167–185 (2016).
20. Zhu, M. et al. Biosynthesis of the nematode attractant 2-Heptanone and its Co-evolution between the pathogenic bacterium *Bacillus* nematocidal and Non-pathogenic bacterium *Bacillus subtilis*. *Front. Microbiol.* **2**, 10:1489 (2019).
21. Sagasti, A., Hobert, O., Troemel, E. R., Ruvkun, G. & Bargmann, C. I. Alternative olfactory neuron fates are specified by the LIM homeobox gene lim-4. *Genes Dev.* **13** (14), 1794–1806 (1999).
22. Bargmann, C. I. & Chemosensation in *C. elegans*. *WormBook: Online Rev. C Elegans Biology* 1–29 (2006).
23. Zhang, C. et al. The olfactory signal transduction for attractive odorants in *Caenorhabditis elegans*. *Biotechnol. Adv.* **32** (2), 290–295 (2014).
24. Zhang, C. et al. The signaling pathway of *Caenorhabditis elegans* mediates chemotaxis response to the attractant 2-Heptanone in a Trojan Horse-like pathogenesis. *J. Biol. Chem.* **291** (45), 23618–23627 (2016).
25. Zhu, M. et al. Multiple olfactory pathways contribute to the lure process of *Caenorhabditis elegans* by pathogenic bacteria. *Sci. China Life Sci.* **64** (8), 1346–1354 (2021).
26. Sattler, R. & Tymianski, M. Molecular mechanisms of calcium-dependent excitotoxicity. *J. Mol. Med.* **78** (1), 3–13 (2000).
27. Thurston, T. L., Wandel, M. P., von Muhlinen, N., Foeglein, A. & Randow, F. Galectin 8 targets damaged vesicles for autophagy to defend cells against bacterial invasion. *Nature* **482** (7385), 414–418 (2012).
28. Maejima, I. et al. Autophagy sequesters damaged lysosomes to control lysosomal biogenesis and kidney injury. *EMBO J.* **32** (17), 2336–2347 (2013).
29. Lomenick, B., Jung, G., Wohlschlegel, J. A. & Huang, J. Target identification using drug affinity responsive target stability (DARTS). *Curr. Protocols Chem. Biol.* **3** (4), 163–180 (2011).
30. Skrott, Z. et al. Alcohol-abuse drug Disulfiram targets cancer via p97 Segregase adaptor NPL4. *Nature* **552** (7684), 194–199 (2017).
31. Li, Y. et al. *elegans*-based screen identifies lysosome-damaging alkaloids that induce STAT3-dependent lysosomal cell death. *Protein Cell.* **9** (12), 1013–1026 (2018).
32. Fehrenbacher, N. et al. Jäättelä M. Sensitization to the lysosomal cell death pathway by oncogene-induced down-regulation of lysosome-associated membrane proteins 1 and 2. *Cancer Res.* **68** (16), 6623–6633 (2008).
33. Kirkegaard, T. et al. Hsp70 stabilizes lysosomes and reverts Niemann-Pick disease-associated lysosomal pathology. *Nature* **463** (7280), 549–553 (2010).
34. Blok, V. C., Jones, J. T., Phillips, M. S. & Trudgill, D. L. Parasitism genes and host range disparities in biotrophic nematodes: The conundrum of polyphagy versus specialisation. *BioEssays News Rev. Mol. Cell. Dev. Biol.* **30** (3), 249–259 (2008).
35. Caboni, P., Ntalli, N. G., Aissani, N., Cavoski, I. & Angioni, A. Nematicidal activity of (E, E)-2,4-decadienal and (E)-2-decenal from *Ailanthus altissima* against *Meloidogyne Javanica*. *J. Agric. Food Chem.* **60** (4), 1146–1151 (2012).
36. Chen, J. et al. A novel *Meloidogyne graminicola* effector, MgGPP, is secreted into host cells and undergoes glycosylation in concert with proteolysis to suppress plant defenses and promote parasitism. *PLoS Pathog.* **13** (4), e1006301 (2017).
37. Rutter, W. B., Franco, J. & Gleason, C. Rooting out the mechanisms of Root-Knot Nematode-Plant interactions. *Annu. Rev. Phytopathol.* **60**, 43–76 (2022).
38. Luo, T., Hou, S., Yang, L., Qi, G. & Zhao, X. Nematodes avoid and are killed by *Bacillus mycoides*-produced styrene. *J. Invertebr. Pathol.* **159**, 129–136 (2018).
39. Eskelinen, E. L. et al. Saftig P. Role of LAMP-2 in lysosome biogenesis and autophagy. *Mol. Biol. Cell.* **13** (9), 3355–3368 (2002).
40. Bohnert, K. A. & Kenyon, C. A lysosomal switch triggers proteostasis renewal in the immortal *C. elegans* germ lineage. *Nature* **551** (7682), 629–633 (2017).
41. Syntichaki, P., Samara, C. & Tavernarakis, N. The vacuolar H+ -ATPase mediates intracellular acidification required for neurodegeneration in *C. elegans*. *Curr. Biol. CB.* **15** (13), 1249–1254 (2005).
42. Petersen, N. H. et al. Transformation-associated changes in sphingolipid metabolism sensitize cells to lysosomal cell death induced by inhibitors of acid Sphingomyelinase. *Cancer Cell.* **24** (3), 379–393 (2013).
43. Yamashima, T. & Oikawa, S. The role of lysosomal rupture in neuronal death. *Prog. Neurobiol.* **89** (4), 343–358 (2009).
44. Yamashima, T. Can 'calpain-cathepsin hypothesis' explain alzheimer neuronal death? *Ageing Res. Rev.* **32**, 169–179 (2016).
45. Lee, S. K., Li, W., Ryu, S. E., Rhim, T. & Ahnn, J. Vacuolar (H+)-ATPases in caenorhabditis elegans: What can we learn about giant H + pumps from tiny worms? *Biochim. Biophys. Acta.* **1797** (10), 1687–1695 (2010).
46. Ahn, D. H., Singaravelu, G., Lee, S., Ahnn, J. & Shim, Y. H. Functional and phenotypic relevance of differentially expressed proteins in calcineurin mutants of *Caenorhabditis elegans*. *Proteomics* **6** (4), 1340–1350 (2006).
47. Brenner, S. The genetics of *Caenorhabditis elegans*. *Genetics* **77** (1), 71–94 (1974).
48. Coburn, C. et al. Anthranilate fluorescence marks a calcium-propagated necrotic wave that promotes organismal death in *C. elegans*. *PLoS Biol.* **11** (7), e1001613 (2013).
49. Treusch, S. et al. *Caenorhabditis elegans* functional orthologue of human protein h-mucolipin-1 is required for lysosome biogenesis. *Proc. Natl. Acad. Sci. U.S.A.* **101** (13), 4483–4488 (2004).
50. Hinas, A., Wright, A. J. & Hunter, C. P. SID-5 is an endosome-associated protein required for efficient systemic RNAi in *C. elegans*. *Curr. Biol. CB.* **22** (20), 1938–1943 (2012).
51. Chin, R. M. et al. Monsalve G. C. The metabolite α-ketoglutarate extends lifespan by inhibiting ATP synthase and TOR. *Nature* **510** (7505), 397–401 (2014).
52. Wong, S. H. Cloning of flavin reductase into pET32a (+) expression vector lacking the thioredoxin A Tag to study solubility of EDTA monooxygenase A in overexpression systems. *J. Exp. Microbiol. Immunol.* **8**, 59–66 (2005).
53. Butt, T. R., Edavettal, S. C., Hall, J. P. & Mattern, M. R. SUMO fusion technology for difficult-to-express proteins. *Protein Exp. Purif.* **43** (1), 1–9 (2005).
54. Jerabek-Willemsen, M., Wienken, C. J., Braun, D., Baaske, P. & Duhr, S. Molecular interaction studies using microscale thermophoresis. *Assay Drug Dev. Technol.* **9** (4), 342–353 (2011).
55. Kamath, R. S. & Ahringer, J. Genome-wide RNAi screening in *Caenorhabditis elegans*. *Methods (San Diego Calif).* **30** (4), 313–321 (2003).
56. Luke, C. J. et al. An intracellular Serpin regulates necrosis by inhibiting the induction and sequelae of lysosomal injury. *Cell* **130** (6), 1108–1119 (2007).
57. Liu, B., Du, H., Rutkowski, R., Gartner, A. & Wang, X. LAAT-1 is the lysosomal lysine/arginine transporter that maintains amino acid homeostasis. *Sci. (New York N. Y.).* **337** (6092), 351–354 (2012).
58. He, X., Chen, F., Dagan, A., Gatt, S. & Schuchman, E. H. A fluorescence-based, high-performance liquid chromatographic assay to determine acid Sphingomyelinase activity and diagnose types A and B Niemann-Pick disease. *Anal. Biochem.* **314** (1), 116–120 (2003).
59. Luo, L. et al. Determination of acid Sphingomyelinase activity in biological samples with ultra-performance liquid chromatographic assay. *J. Liq. Chromatogr. Relat. Technol.* **41**, 855–859 (2018).

Author contributions

W.D. and Y.Z. conducted the experiment(s). W.D. and Y.Z. wrote the main manuscript text. F. Y. ,W. C., C. L. and Y. T. analysed the results. F. H., M. C., L. Z.and W. C. commented on the manuscript. W.C. and J. Z. edited and reviewed the manuscript. All authors contributed critically to the drafts and gave final approval for publication.

Funding

This research was supported by the National Nature Science Foundation of China (32200041); the National Nature Science Foundation of China (32100043).

Declarations

Competing interests

The authors declare no competing interests.

Additional information

Supplementary Information The online version contains supplementary material available at https://doi.org/10.1038/s41598-025-95332-z.

Correspondence and requests for materials should be addressed to J.Z.

Reprints and permissions information is available at www.nature.com/reprints.

Publisher's note Springer Nature remains neutral with regard to jurisdictional claims in published maps and institutional affiliations.